

Measurement of Direct Photon Emission in $K^+ \rightarrow \pi^+ \pi^0 \gamma$ Decay

S. Adler,¹ M. Aoki,^{5,*} M. Ardebili,⁴ M. S. Atiya,¹ P. C. Bergbusch,^{5,7} E. W. Blackmore,⁵ D. A. Bryman,^{5,7} I.-H. Chiang,¹ M. R. Convery,⁴ M. V. Diwan,¹ J. S. Frank,¹ J. S. Haggerty,¹ T. Inagaki,² M. M. Ito,⁴ S. Kabe,² S. H. Kettell,¹ Y. Kishi,³ P. Kitching,⁶ M. Kobayashi,² T. K. Komatsubara,² A. Konaka,⁵ Y. Kuno,² M. Kuriki,² T. F. Kycia,^{1,†} K. K. Li,¹ L. S. Littenberg,¹ J. A. Macdonald,⁵ R. A. McPherson,⁴ P. D. Meyers,⁴ J. Mildenerberger,⁵ N. Muramatsu,² T. Nakano,⁵ T. Numao,⁵ J.-M. Poutissou,⁵ R. Poutissou,⁵ G. Redlinger,^{5,‡} T. Sato,² T. Shinkawa,² F. C. Shoemaker,⁴ R. Soluk,⁶ J. R. Stone,⁴ R. C. Strand,¹ S. Sugimoto,² C. Witzig,¹ and Y. Yoshimura²
(E787 Collaboration)

¹Brookhaven National Laboratory (BNL), Upton, New York 11973

²High Energy Accelerator Research Organization (KEK), Oho, Tsukuba, Ibaraki 305-0801, Japan

³RCNP, Osaka University, 10-1 Mihogaoka, Ibaraki, Osaka 567-0047, Japan

⁴Joseph Henry Laboratories, Princeton University, Princeton, New Jersey 08544

⁵TRIUMF, 4004 Wesbrook Mall, Vancouver, British Columbia, Canada V6T 2A3

⁶Centre for Subatomic Research, University of Alberta, Edmonton, Alberta, Canada T6G 2N5

⁷Department of Physics and Astronomy, University of British Columbia, Vancouver, British Columbia, Canada V6T 1Z1

(Received 13 July 2000)

We have performed a measurement of the $K^+ \rightarrow \pi^+ \pi^0 \gamma$ decay and have observed 2×10^4 events. The best fit to the decay spectrum gives a branching ratio for direct photon emission of $(4.7 \pm 0.8 \pm 0.3) \times 10^{-6}$ in the π^+ kinetic energy region of 55 to 90 MeV and requires no component due to interference with inner bremsstrahlung.

PACS numbers: 13.20.Eb, 12.39.Fe, 13.40.Ks

The radiative decay $K^+ \rightarrow \pi^+ \pi^0 \gamma$ ($K_{\pi^2\gamma}$) in which the γ is directly emitted (DE) is sensitive to important aspects of the low energy hadronic interactions of mesons [1]. Although the DE component is difficult to observe because it is very small compared to the dominant inner bremsstrahlung (IB) associated with the $K^+ \rightarrow \pi^+ \pi^0$ (K_{π^2}) decay, it may be isolated kinematically. The DE component consists of magnetic and electric transitions. At $O(p^4)$ in chiral perturbation theory (ChPT), the magnetic amplitude consists of a reducible amplitude [2] which is unambiguously determined by the Wess-Zumino-Witten functional [3] with a chiral anomaly and of a direct anomalous amplitude [4], arising from chirally covariant odd-parity octet operators. The direct anomalous amplitude is not calculable in a model-independent way but the size is expected to be comparable to that of the reducible amplitude or smaller. At $O(p^6)$ in ChPT, vector meson exchange (VME) contributions are also possible but, in contrast to the $K_L \rightarrow \pi^+ \pi^- \gamma$ decay [5], the VME contributions are less important; a weak deformation model [6] predicts that the VME and the direct $O(p^6)$ contributions cancel [2]. There is no definite prediction from ChPT of the electric transition amplitude, which depends on undetermined constants. Since the electric amplitude interferes (INT) with the IB amplitude, it may be distinguished from the magnetic amplitude, which does not. The experimental determination of the electric amplitude is of great interest, not only for ChPT, but for searches for possible non-standard-model effects like a CP -violating asymmetry between $K^+ \rightarrow \pi^+ \pi^0 \gamma$ and $K^- \rightarrow \pi^- \pi^0 \gamma$ decay widths predicted in supersymmetry [7].

Previous experiments [8–10] used decay-in-flight techniques to measure the $K_{\pi^2\gamma}$ branching ratio in the π^+ kinetic energy region $55 \text{ MeV} < T_+ < 90 \text{ MeV}$ with Abrams *et al.* [8] confirming the theoretical prediction for the IB branching ratio of 2.61×10^{-4} [1]. The current Particle Data Group average for the DE component of the branching ratio is $(1.8 \pm 0.4) \times 10^{-5}$ [11], which is 5 times larger than calculated from the reducible anomalous amplitude alone and is consistent with the coherent combination of that amplitude and the direct anomalous amplitude suggested by a factorization model [4]. A decay spectrum shape analysis of Ref. [8] indicates the absence of electric contributions to the DE component but the existing data are not precise enough to rule out constructive interference with IB.

The differential decay width for the decay $K^+(p) \rightarrow \pi^+(p_+) \pi^0(p_0) \gamma(q)$ is conveniently expressed in terms of a Lorentz invariant variable $W^2 \equiv (p \cdot q)(p_+ \cdot q)/(m_{\pi^+}^2 m_K^2)$, where p , p_+ , and q are 4-momenta of the K^+ , π^+ , and γ , and m_{π^+} and m_K are masses of π^+ and K^+ , respectively. The differential width can be written in terms of the IB differential width as

$$\frac{\partial^2 \Gamma}{\partial T_+ \partial W} = \frac{\partial^2 \Gamma_{\text{IB}}}{\partial T_+ \partial W} \left[1 + 2 \frac{m_{\pi^+}^2}{m_K} \text{Re} \left(\frac{E}{eA} \right) W^2 + \frac{m_{\pi^+}^2}{m_K^2} \left(\left| \frac{E}{eA} \right|^2 + \left| \frac{M}{eA} \right|^2 \right) W^4 \right], \quad (1)$$

where T_+ is the kinetic energy of the charged pion in the kaon rest frame, A is the decay amplitude for $K^+ \rightarrow \pi^+ \pi^0$, and E and M are electric and magnetic DE amplitudes, respectively. The direct emission amplitudes E and

M are independent of W and their effects are detectable only in the large W region, while the IB decay amplitude is proportional to $1/W^2$ and thus dominates in the small W region. Experimental determination of these amplitudes requires high sensitivity to deviations of the measured spectrum from that of IB over a wide W region.

The E787 detector [12] at the Alternating Gradient Synchrotron (AGS) of Brookhaven National Laboratory (BNL) was used to study $K_{\pi 2\gamma}$. Kaons of 790 MeV/ c [13] were incident on a solenoidal spectrometer with a 1.0 T field at a rate of 7×10^6 per 1.6-s spill of the AGS. The spectrometer contains beam detectors, a scintillating-fiber target where the kaons stop and decay, a central cylindrical drift chamber, and a range stack (RS) of plastic scintillators with embedded straw chambers. Measurements of momentum, kinetic energy and range of charged decay products were performed. The output pulse shapes of the RS counters were recorded, providing good timing accuracy. A hermetic calorimeter system consisting of barrel (BL) and end cap (EC) detectors measured the positions and energies of photons and other particles from K^+ decays.

The BL calorimeter was used to detect the three γ 's in the $K_{\pi 2\gamma}$ decay. It consisted of 48 azimuthal sectors and 4 radial layers of sandwiches of lead (1 mm) and plastic scintillator (5 mm) sheets, 14 radiation lengths in depth covering a solid angle of about 3π sr. The visible fraction of the energy deposited in this system was 30%. The Z position (along the beam axis) of the BL hits was obtained using the charge and timing information from phototubes on both ends of the 2-m long modules.

The trigger for $K_{\pi 2\gamma}$ required a K^+ decay at rest, a charged track in a kinetic energy region between the end point of the $K^+ \rightarrow \pi^+ \pi^0 \pi^0$ ($K_{\pi 3}$) decay and the peak of the $K_{\pi 2}$ decay, at least three BL clusters, no extra particles in the RS, and no energy in the EC. The total number of kaon decays at rest available for the $K_{\pi 2\gamma}$ study was 1.8×10^{11} , and a total of 1.1×10^7 events survived the trigger. Most of them were due to $K^+ \rightarrow \pi^0 \mu^+ \nu_\mu$ ($K_{\mu 3}$), $K^+ \rightarrow \pi^0 e^+ \nu_e$ ($K_{e 3}$), and $K_{\pi 2}$.

The momentum vector, the kinetic energy, and the range of the charged particle were successfully reconstructed and measured with the target, the drift chamber, and the RS (7.7×10^6 events). To remove $K_{\pi 2}$ events, the momentum was required to be less than 195 MeV/ c (6.3×10^6 events). Energy-momentum and range-momentum consistency were imposed to reject $K_{e 3}$ decays and events with the pion range shortened by nuclear interactions or by escape from an end of the RS (2.2×10^6 events). The energy and direction of the three γ 's were determined from reconstruction of the BL hits and the K^+ decay vertex position in the target (1.3×10^6 events). Events with a missing momentum squared greater than $(100 \text{ MeV}/c)^2$ were rejected to reduce background events with an energetic neutrino (5.4×10^5 events). The major background to the $K_{\pi 2\gamma}$ decay was $K_{\mu 3}$. Consistency between the range measured

in the RS and the momentum measured in the drift chamber was imposed to reject μ^+ backgrounds while retaining 92% of the signal (1.2×10^5 events). Events were also rejected based on the presence of any activity additional to three γ 's and a π^+ (8.7×10^4 events).

A kinematic fit was applied to 13 observables (the kinetic energy and momentum vector of the charged particle, and momentum vectors of three γ 's) with the following six constraints: total energy-momentum conservation, consistency of the charged particle's energy and momentum with a pion hypothesis, and invariant mass of two γ 's being equal to m_{π^0} . Since there are three possible pairings of the γ 's to form the π^0 , incorrect pairing can move IB events into the region of large W although IB events tend to populate the region of small W .

To minimize the contamination arising from a wrong combination, the square of the matrix element of the IB decay was taken as a weight in the selection of the two γ 's to be assigned to the π^0 , and the combination which maximized the product of the χ^2 probability of the kinematic fit, $\text{Prob}(\chi^2)$, and the IB weight were chosen among the three possible event topologies. Figure 1 shows the χ^2 probability distribution of the fitted events. The distribution indicates that the measurement resolution is properly accounted for throughout all values of W . Most of events at $\text{Prob}(\chi^2) = 0$ are due to pion nuclear interactions and muon background, which do not satisfy the kinematic constraints.

In the Monte Carlo simulation of the IB, DE, and INT spectra, $K_{\pi 2\gamma}$ events were generated with the corresponding matrix elements in [1] and analyzed with the code used for real data. Thus, the effect of possible incorrect pairing of the two γ 's from π^0 on the Monte Carlo spectra was taken into account. The probability of incorrect pairing with this analysis was estimated to be 2.6% for IB, 20% for DE,

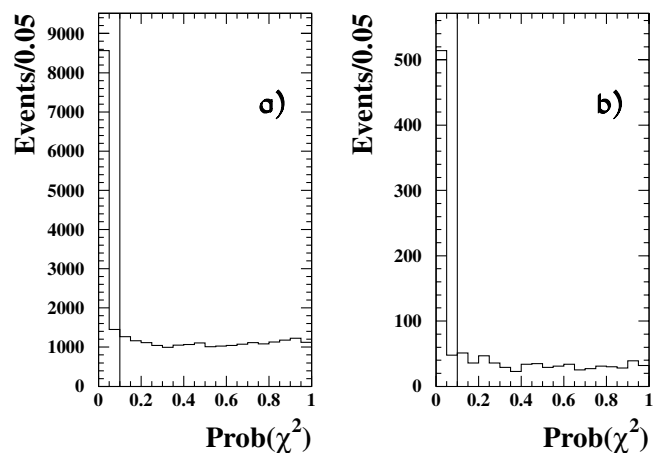


FIG. 1. Distribution of the χ^2 probability for the fitted events. Events with $\text{Prob}(\chi^2) \geq 0.1$ are accepted as due to $K^+ \rightarrow \pi^+ \pi^0 \gamma$ decay. All selection cuts except for the $\text{Prob}(\chi^2)$ cut are applied. (a) All events. (b) Events in a region of $W > 0.5$.

and 9% for INT. For IB, 2.3% of the events populate the region of $W > 0.5$, and only 6% of them were due to incorrect pairing. The estimated W resolution was about 0.02.

For the signal selection we required the χ^2 probability to be greater than 10% (4.5×10^4 events) and the fitted π^+ momentum to be between 140 and 180 MeV/c (3.4×10^4 events); the latter condition on π^+ momentum was imposed to remove the $K\pi_3$ and $K\pi_2$ backgrounds as well as $K^+ \rightarrow \pi^+\pi^0\gamma$ decays outside the region $55 \text{ MeV} < T_+ < 90 \text{ MeV}$. For the γ 's, we required the measured energies to be greater than the on-line threshold energy (3.0×10^4 events), the fitted energies to be at least 20 MeV (2.3×10^4 events), and the $\cos\theta_\gamma$'s to be smaller than 0.6, where θ_γ is the fitted polar angle of a γ with respect to the beam (2.1×10^4 events). Events with $W < 0.1$ were not used for a shape analysis. A total of 19 836 events survived all selection cuts, 8 times more than the previous experiments. Figure 2a shows the π^+ momentum distribution of the $K\pi_2\gamma$ events after applying all selection cuts. The π^+ momentum distribution is insensitive to the DE contribution, and thus it is reproduced by a Monte Carlo simulation of the IB contribution alone. Figure 2b shows the invariant $\gamma\gamma$ mass distribution of the π^0 from the same events.

Figure 3a shows the W projection of the signal events in the T_+ signal region. The dashed curve is a best fit to IB alone with a χ^2 of 61 for 7 degrees of freedom. The solid curve is the best fit to the sum of IB and DE and gives a χ^2 of 7.9 for 6 degrees of freedom. Normalized to the IB spectrum the deviation of the measured spectrum at large W is shown in Fig. 3b. The DE component was measured to be $(1.8 \pm 0.3)\%$ of the IB component in the region $55 \text{ MeV} < T_+ < 90 \text{ MeV}$. The branching ratio for DE is determined to be $B^{T_+}(\text{DE}) = (4.7 \pm 0.8) \times 10^{-6}$

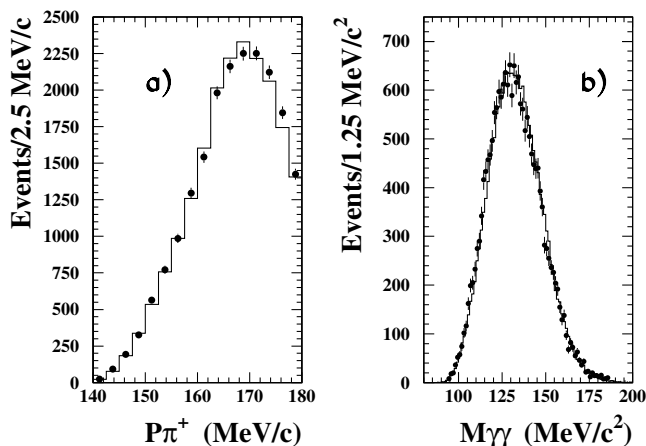


FIG. 2. (a) Momentum distribution of observed π^+ events (dots) and Monte Carlo simulation with IB alone (solid histogram). A χ^2 of the fit is 18 for 15 degrees of freedom. (b) Invariant $\gamma\gamma$ mass distribution (dots) and Monte Carlo simulation with IB alone (solid histogram). A pairing which gives an invariant mass closest to the π^0 mass was selected among three possible pairings.

in the T_+ signal region by normalizing to the theoretical prediction for the IB branching ratio. The best fit to the sum of IB, DE, and INT gives the INT component to be $(-0.4 \pm 1.6)\%$ of the IB component with a χ^2 of 7.8 for 5 degrees of freedom. We conclude that no interference term is required for the fit to this spectrum.

Several checks to verify the result were made. Shape analyses were performed on the $\cos\theta_{\pi^+\gamma}$ distribution, where $\theta_{\pi^+\gamma}$ is the opening angle between a π^+ and the radiated γ , and on the energy distribution of the radiated γ . The resulting branching ratios obtained for DE are consistent with the W fitting result to within 3%. This difference is used as an estimator of the systematic error due to the fitting method. Selection of γ pairs without IB weighting reduced the branching ratio by 6% while doubling the statistical uncertainty. Systematic uncertainties due to calibration and resolution of the energy and position measurements were estimated from the observed DE branching ratio variation as each corresponding Monte Carlo parameter was varied over an expected range. The uncertainty due to limited Monte Carlo statistics was estimated by performing the analysis with small subsets of the Monte Carlo data. All systematic uncertainties in the DE branching ratio were added in quadrature to obtain an overall relative error of $\pm 6\%$ ($\pm 0.3 \times 10^{-6}$). Table I gives a summary of the systematic uncertainties.

Two other possible background sources in the large W region are $K^+ \rightarrow \pi^0\mu^+\nu_\mu$ decay with a radiated or accidental γ , and $K\pi_3$ decay with a charged pion decay in flight. Both processes contain a charged muon in the final state. The estimated number of the muon background events was 103 in the whole W region (7 out of a total of 597 with $W > 0.5$), which was obtained by selecting events with a muonlike range-momentum relation. Imposing additional pion identification criteria based on the presence of a $\pi^+ \rightarrow \mu^+\nu$ decay signal in the stopping counter [12] did not change the W spectrum. The insensitivity of

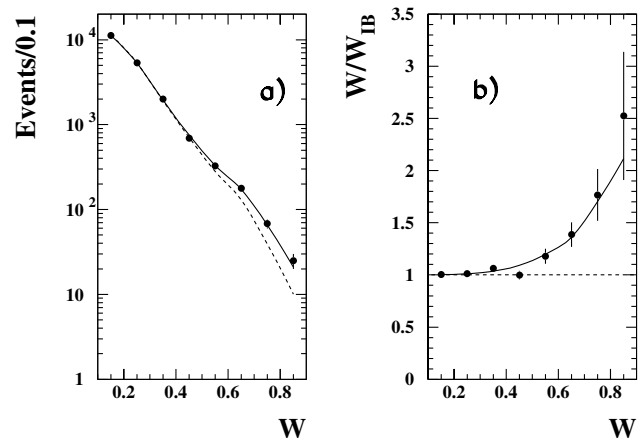


FIG. 3. (a) W spectrum of the observed events and best fits to IB + DE (solid curve) and IB alone (dashed curve). (b) Measured W spectrum normalized to the IB spectrum.

TABLE I. A summary of estimated systematic uncertainties. All uncertainties are added in quadrature to get the total.

Estimated systematic uncertainties	(%)
Fitting method	± 3
π^+ Momentum calibration	$^{+3}_{-1}$
γ Position calibration	$^{+3}_{-0}$
γ Position resolution	$^{+3}_{-0}$
γ Energy calibration	± 0.3
Monte Carlo statistics	± 2
γ Interaction in material	$^{+0}_{-4}$
Total systematic error	± 6

the final result to the variation of photon veto cuts also confirmed that these backgrounds are negligible. Note that $K_{\pi^2\gamma}$ is the most copious K^+ decay emitting a π^+ in the momentum region 140–180 MeV/ c . It is also that most copious K^+ decay with any charged track in the signal momentum region that is accompanied by more than two γ 's.

Assuming a pure magnetic transition for the DE amplitude, the result for $B^{T^+}(\text{DE})$ gives $|M| = (2.1 \pm 0.2) \times 10^{-7}$ for the dimensionless magnetic amplitude in Eq. (1). The reducible anomalous amplitude $|-eG_8 m_K^3 / 2\pi^2 f|$ in Ref. [2] is $|M| = 1.8 \times 10^{-7}$ with standard $O(p^2)$ ChPT coupling constants, $f = 93$ MeV and $|G_8| = 9 \times 10^{-6}$ GeV $^{-2}$. This result supports the hypothesis that the dominant contribution to DE is due to the reducible anomalous amplitude and the other magnetic contributions are small or cancel. Similarly, the null measurement of the INT component gives a 68% confidence-level interval of $-2.6 \times 10^{-8} < \text{Re}(E) < 1.6 \times 10^{-8}$ for the electric amplitude.

In conclusion, we have performed a new measurement of the $K^+ \rightarrow \pi^+ \pi^0 \gamma$ decay with significantly higher statistics and improved kinematic constraints, using the E787 detector and K^+ decays at rest. The branching ratio for the direct emission is $[4.7 \pm 0.8(\text{stat}) \pm 0.3(\text{syst})] \times 10^{-6}$. The decay spectrum indicates that the direct emission amplitude is consistent with being due to purely magnetic contributions comparable to the reducible anomalous contribution.

We gratefully acknowledge the dedicated effort of the technical staff supporting this experiment and of the BNL AGS Department. This research was supported in part by the U.S. Department of Energy under Contracts No. DE-AC02-98CH10886, No. W-7405-ENG-36, and Grant No.

DE-FG02-91ER40671, by the Ministry of Education, Science, Sports and Culture of Japan through the Japan–U.S. Cooperative Research Program in High Energy Physics and under the Grant-in-Aids for Scientific Research, for Encouragement of Young Scientists and for JSPS Fellows, and by the Natural Sciences and Engineering Research Council and the National Research Council of Canada.

*Present address: KEK, Oho, Tsukuba, Ibaraki 305-0801, Japan.

†Deceased.

‡Present address: BNL, Upton, NY 11973.

- [1] G. D'Ambrosio, M. Miragliuolo, and P. Santorelli, in *DAΦNE Physics Handbook*, edited by L. Maiani, G. Panzeri, and N. Paver (Laboratori Nazionali di Frascati, Frascati, 1992); G. Ecker, H. Neufeld, and A. Pich, Nucl. Phys. **B413**, 321 (1994); G. D'Ambrosio and G. Isidori, Z. Phys. C **65**, 649 (1995).
- [2] G. Ecker, H. Neufeld, and A. Pich, Phys. Lett. B **278**, 337 (1992).
- [3] J. Wess and B. Zumino, Phys. Lett. **37B**, 95 (1971); E. Witten, Nucl. Phys. **B223**, 422 (1983).
- [4] J. Bijnens, G. Ecker, and A. Pich, Phys. Lett. B **286**, 341 (1992).
- [5] E. J. Ramberg *et al.*, Phys. Rev. Lett. **70**, 2525 (1993); Y. C. R. Lin and G. Valencia, Phys. Rev. D **37**, 143 (1988).
- [6] G. Ecker, A. Pich, and E. de Rafael, Phys. Lett. B **237**, 481 (1990).
- [7] G. Colangelo, G. Isidori, and J. Portolés, Phys. Lett. B **470**, 134 (1999).
- [8] R. J. Abrams *et al.*, Phys. Rev. Lett. **29**, 1118 (1972).
- [9] K. M. Smith *et al.*, Nucl. Phys. **B109**, 173 (1976).
- [10] V. N. Bolotov *et al.*, Sov. J. Nucl. Phys. **45**, 1023 (1987).
- [11] Particle Data Group, C. Caso *et al.*, Eur. Phys. J. C **3**, 1 (1998).
- [12] M. S. Atiya *et al.*, Nucl. Instrum. Methods Phys. Res., Sect. A **321**, 129 (1992); M. S. Atiya *et al.*, Nucl. Instrum. Methods Phys. Res., Sect. A **279**, 180 (1989); I.-H. Chiang *et al.*, IEEE Trans. Nucl. Sci. **42**, 394 (1995); D. A. Bryman *et al.*, Nucl. Instrum. Methods Phys. Res., Sect. A **396**, 394 (1997); E. W. Blackmore *et al.*, Nucl. Instrum. Methods Phys. Res., Sect. A **404**, 295 (1998); T. K. Komatsubara *et al.*, Nucl. Instrum. Methods Phys. Res., Sect. A **404**, 315 (1998); S. Adler *et al.*, Phys. Rev. Lett. **79**, 2204 (1997); S. Adler *et al.*, Phys. Rev. Lett. **84**, 3768 (2000).
- [13] J. Doornbos *et al.*, Nucl. Instrum. Methods Phys. Res., Sect. A **444**, 546 (2000).